Polymer Bulletin (2023) 80:2485–2501
https://doi.org/10.1007/s00289-022-04173-7

ORIGINAL PAPER

Mechanical properties, thermal behavior, miscibility and light stability of the poly(butylene adipate-co-terephthalate)/poly(propylene carbonate)/polylactide mulch films

Xiangyu Wang[1,2] · Hongwei Pan[1] · Shiling Jia[1] · Zifeng Lu[1,2] · Lijing Han[1] · Huiliang Zhang[1,2,3]

Received: 7 November 2021 / Revised: 2 February 2022 / Accepted: 25 February 2022 /
Published online: 13 March 2022

Abstract

Poly(butylene adipate-co-terephthalate) (PBAT) copolyester, which has good processing properties, is a new biodegradable synthetic polymer material in recent years. However, it is not satisfied with the mulch requirements because of its high cost and low mechanical strength. The mulch films of ternary blends including PBAT, polylactide (PLA), and poly(propylene carbonate) (PPC) are successfully prepared by extrusion blending and film blowing. The effect of different blow-up ratios (BUR) on the mechanical of mulch films was investigated. The 64/20/16 wt% PBAT/PPC/PLA mulch film of 3.1 BUR shows good mechanical properties. The tensile strength is as high as 43.0/37.6 MPa (MD/TD) while the elongation at break reaches 160/450% (MD/TD). The addition of PLA improves the strength of the mulch film, and the addition of PPC improves the barrier performance of the mulch film. It demonstrates that the PBAT, PPC, and PLA have partial compatibility from DMA and DSC analysis. After adding high-efficiency hindered amine light stabilizers, the mulch films have good light stability and their elongation at the break still exceeds 100% after 100 h of UV irradiation.

Keywords Poly(butylene adipate-co-terephthalate) · Polylactide · Poly(propylene carbonate) · Mulch films · Biodegradability

✉ Lijing Han
ljhan@ciac.ac.cn

✉ Huiliang Zhang
hlzhang@ciac.ac.cn

[1] Key Laboratory of Polymer Ecomaterials, Chinese Academy of Sciences, Changchun Institute of Applied Chemistry, Changchun 130022, China

[2] University of Science and Technology of China, Hefei 230026, China

[3] Zhejiang Zhongke Applied Chemistry Technology Co., Ltd., Hangzhou 310000, China

Introduction

Plastic agricultural mulch film is an essential part of agriculture. It can increase soil temperature, maintain soil moisture and fertility, prevent pests from attacking crops, promote plant growth, and increase crop yield. Polyethylene (PE) is widely used in mulch films. High-density polyethylene resins (HDPE) have reliable moisture and vapor barriers. Low-density polyethylene resins (LDPE) have high puncture resistance and mechanical stretch properties, and LDPE is mainly used in agricultural mulch films. However, PE is extremely difficult to degrade, and the degradation cycle can reach hundreds of years. Moreover, after the aging and broken mulching film, the residual film is not easy to degrade and recycle in the land. Prolonged use of this type of mulch can cause long-term damage to the ground that is difficult to resolve [1–3]. In recent years, in order to solve the pollution problem caused by non-degradable plastics, biodegradable polymers have been widely studied. It can be used to replace other plastics in various fields, such as food packaging, biomedicine, and agricultural mulch film. [4–9]

The poly(butylene adipate-co-terephthalate) (PBAT), poly(propylene carbonate) (PPC), polylactide (PLA), thermoplastic starch, polyhydroxyalkanoates, and poly(butylene succinate) have received considerable attention for their use in plastic mulch films [3]. Among these polymers, PBAT and PLA are more utilized. PBAT is a thermoplastic biodegradable plastic synthesized with petroleum-based raw materials. It is a copolymer of aliphatic butylene adipate and aromatic butylene terephthalate, which combines aliphatic polyester and aromatic polyester. It has good ductility, stretchability and also has good impact resistance and heat resistance. It is similar to LDPE in processing and mechanical properties, so it is currently the most promising alternative to polyvinyl material [10, 11]. PLA, as a biodegradable polymer, has high strength, good biocompatibility, and transparency. However, PLA is brittleness and has poor impact resistance [12–15]. The PBAT/PLA blend film is particularly eye-catching due to its high-strength and high-toughness complementary properties, which have the substantial commercial potential [16–21]. Chiu et al. showed that adding 30 wt% of PBAT to PLA could increase the elongation at break from 3.0% to about 25.0%, and reduce the tensile strength from 58.0 to 43.0 MPa [18]. PPC is an entirely degradable, environmentally friendly plastic synthesized by the alternating copolymerization of propylene oxide and carbon dioxide. PPC has pretty good barrier properties. But it has poor mechanical properties and weak heat resistance. It usually cannot be used alone and is often used in blending and modifying with other materials [22–25].

During the use of mulch films in the field, they will be exposed to solar radiation, especially ultraviolet rays, which can cause photodegradation, damage mechanical properties and product efficiency, and make it challenging to prevent weeds from growing [26–28]. Therefore, the role of light stabilization cannot be ignored. Hindered Amine Light Stabilizers (HALS) can be applied in PBAT blend mulches [29]. Souza et al. pointed out that the presence of HALS is very important for reducing chain scission caused by ultraviolet radiation. Toxicological

tests pointed out that after adding HALS to PBAT, no substances harmful to the human body were detected after soil burial degradation [30, 31].

To obtain better mechanical properties, choosing appropriate process parameters in blown film manufacture is indispensable. As all we know, the blow-up ratio (BUR) is the most important process parameter in the process of blown films formation. Therefore, PBAT/PPC/PLA ternary mulch films were prepared as a function of different BUR by extrusion blending and blow molding. HALS UV-770 was used to improve the light stability of the mulch film. The mechanical properties, compatibility, thermal behaviour, barrier performance and light stability of the PBAT/PPC/PLA films were investigated in detail.

Materials and methods

Materials

All materials used in the study were commercial grade. PBAT was supplied by Xinjiang Blue Ridge Tunhe Polyester Co., Ltd. (China). The commercial PLA 4032D was purchased from NatureWorks (USA). PPC was supplied by Taizhou Bangfeng Plastic Co., Ltd. (China). Hindered amine light stabilizer (HALS) UV-770 was provided by Nanjing Hua Lim Chemical Co., Ltd. (China) (Scheme 1).

Preparation of the mulch films

Before compounding, PBAT, PPC, PLA, and UV-770 were dried at 50 °C for 24 h. The samples were first blended in a twin-screw extruder with a screw diameter of 20 mm and L/D ratio of 32 and at a rotating speed of 200 rpm. The temperature of the twin-screw extruder was set from 150 to 190 °C. The mixing compositions of the PBAT/PPC/PLA blends were 90/10/0, 90/0/10, 80/20/0, 72/20/8, 72/12/16, 64/28/8, 64/20/16, and 64/12/24 wt%, respectively. And the mixing compositions of the PBAT/PPC/PLA/UV-770 blends were 64/20/16/0, 64/20/16/0.25, 64/20/16/0.5, 64/20/16/0.75, and 64/20/16/1 wt%, respectively. After melt blending, the extrudate was cut into pellets by pelletizing machine after being cooled in a water bath. The extrudate was dried at 80 °C for 8 h. Then, all the samples were compression molded into sheets with thicknesses of 1.0 mm at 185 °C for DMA analysis.

Afterwards, all the PBAT/PPC/PLA and PBAT/PPC/PLA/UV-770 blends were blown using a single-screw extruder with an aspect ratio of 30:1 and were equipped with a 6-inch diameter blown film die. The external cooling air temperature was about 20 °C. The thickness of the film was about 8 μm. The barrel temperature in different zones was independently in the range of 170–190 °C. The screw speed was set to 38 rpm. In the form of a tube, the molten polymer was pulled up from the mold by the device. Moreover, the extruder output was 8 $kg{\cdot}h^{-1}$, the BUR was 1.8, 2.6 and 3.1, respectively. BUR is calculated by the following formula:

Scheme 1. Structure of PBAT, PLA, PPC and UV-770

$$\mathrm{BUR} = \frac{D_1}{D_2} \tag{1}$$

D_1 represents the diameter of bubble film, D_2 is the diameter of the die.

The frost line height (distance from die exit) was about 15 cm, and the winding speed was 12 m·min^{-1}. The thickness of mulch films is controlled in 8–12 μm, the film of neat PLA is about 100 μm. The mechanical properties, thermal properties, barrier properties, morphology of the tear-fracture surfaces of the PBAT/PPC/PLA films were studied. The light stability, ultraviolet aging and light stabilizer mechanism of the PBAT/PPC/PLA/UV-770 films were investigated.

Mechanical Properties

The PBAT/PPC/PLA and PBAT/PPC/PLA/UV-770 mulch films were performed using a tensile testing machine (Instron-1121, Canton, MA) at a cross-head speed of 50 mm/min according to ASTM D882-2010. All tests were at 50% relative humidity and 23 ± 2 °C. At least six specimens were tested for each sample to get an average value.

The right-angle tearing strength was measured on an Instron 1121 testing machine at 23 ± 2 °C. The measurements were conducted at a cross-head speed of 50 mm/min according to QB/T 1130–91 in the machine direction (MD) and the transverse direction (TD), respectively. At least six specimens were tested for each sample to get an average value.

Morphological characterization

The tear fractured surfaces of the PBAT/PPC/PLA mulch films were analyzed by scanning electron microscope (SEM) (Merlin, Zeiss, Germany). The mulch films were installed on a short aluminium plate with conductive paint and sputtered with gold before SEM observation.

Dynamic mechanical analysis (DMA)

DMA of the mulch films was performed in a DMA instrument (DMA 850, TA Instruments, USA) in the tensile mode according to ASTM D4092. The size of the sample was L × W × H = 12 × 4 × 1 mm^3. The temperature ranged from − 60 to 110 °C at a constant heating rate of 3 °C min^{-1} and a frequency of 1 Hz for samples. The amplitude was 10 μm. Before the experiment, the preload was 0.01 N. The storage modulus (E') and loss tangent (tanδ) were tested.

Differential scanning calorimetry (DSC)

Thermal properties of the PBAT/PPC/PLA films were studied by using DSC (DSC Q20, TA Instruments, USA) under nitrogen atmosphere. The weight of the samples varied between 5.0 and 10.0 mg. In the first heating run, the films were heated from

0 to 190 °C at a heating rate of 10 °C·min^{-1} and kept the temperature at 190 °C for 5 min. Then the films were cooled to -50 °C at a 10 °C·min^{-1} cooling rate. In the second heating run, the films were heated again to 190 °C at a 10 °C·min^{-1} heating rate. The degree of crystallization of the sample is evaluated by the following relationship from the heat generated during the crystallization process:

$$x = \frac{\Delta H_m}{\Delta H_m^0 \times W_{\mathrm{PLA}}} \tag{2}$$

where x is the crystallinity of the samples, ΔH_m is the heat of fusion of the PLA in the mulch films, ΔH_m^0 is the heat of fusion of 100% crystallinity PLA (93 J·g^{-1}), and W_{PLA} is the mass fraction of PLA in the mulch films [32].

Water vapour permeability of the Films (WVP)

The water vapour permeability of the PBAT/PPC/PLA films was determined using a water vapour transmission tester (ASTM E96, Labthink, China) according to the ASTM E96-95 standard method. The diameter of the sample was 74 mm. The samples were attached to the aluminium infiltration tank containing anhydrous calcium chloride. The experiment temperature was 25 °C, the humidity was 84 ± 2%, and the experiment time was 48 h. To eliminate the error caused by different film thicknesses, samples with similar thicknesses were selected. The WVP of mulch films was calculated determined by the following equation:

$$\mathrm{WVP} = \frac{\Delta W}{A \times \Delta t} \frac{L}{\Delta P} \tag{3}$$

where ΔW is the weight of permeation samples gained by desiccant (g), A is the permeation area (m^2), Δt is the time of permeation (second), L is the average film thickness (m), and ΔP (Pa) is water partial pressure difference between two sides of the film.

UV aging test

The PBAT/PPC/PLA/UV-770 mulch films were prepared and treated according to GB/T 16,422.1, each sample aged 3 pieces, after the aging of a large sample cut a single sample for testing. The average irradiance is the narrow band (340 nm) 0.51 W·(m^2·nm)$^{-1}$, temperature control using a black label thermometer, the experiment time is 100 h.

Fourier transform infrared spectrometer (FTIR)

Fourier transform infrared spectra were recorded with (Nicolet 6700, USA) spectrometer. All samples were washed with distilled water before the experiment and dried in a vacuum oven at 50 °C for 8 h. The spectra were obtained in the range 400–4000 cm^{-1} with a resolution of 4 cm^{-1} and a scan rate of 8 scans per second.

Results and discussion

Mechanical properties

The effects of different BUR on the mechanical properties of mulch films were studied firstly (Fig. 1). For neat PBAT and neat PLA films, BUR had little effect on tensile strength. The tear strength of MD increased with the increase of BUR, and the tear strength of TD decreased with the increase of BUR. For blend mulch films, the elongation at break of the films decreased slightly with the increase of BUR. And the tensile strength of the films increased with the increase of BUR. This was because BUR corresponded to the transverse expansion multiple of the film. A larger BUR meant a more significant effect on the transverse stretching of the film, which will strengthen the orientation of the molecular chains in TD and increase the tensile strength of the film. For the 64/20/16 PBAT/PPC/PLA mulch films, the tensile strength in TD increased from 26.2 to 37.6 MPa with the increase of BUR. But correspondingly, the orientation of the film in MD was weakened, resulting in a slight decrease in MD tensile strength of the film, from 43.2 to 42.0 MPa. Different BUR has little effect on the tear strength of the blend films. Considering the relatively low tensile strength in TD, the BUR for the most suitable mulch film was 3.1.

The mechanical properties of the PBAT/PPC/PLA films were shown in Table 1 (All the mechanical properties were shown in Table S1, Supporting Information). Combining the advantages of the high strength of PLA and the high toughness of PBAT, the mulch films showed good mechanical properties. Mulch films reflected higher tensile strength in MD and higher elongation at break in TD due to the orientation during the blown film process of the polymer. Generally speaking, the tensile strength in MD is always higher than that in TD. This difference could be ascribed to the parallel orientation of the molecular chain in MD. Tearing rupture was more difficult along with the perpendicular orientation than the parallel orientation of the molecular chain. When the brittle and hard PLA was added, the tensile strength of the mulch film had increased from 40.0 MPa/29.2 MPa (MD/TD) to 49.8 MPa/37.8 MPa, and the elongation at break has decreased from 232.0%/554.6% (MD/TD) to 139.0%/381.3%, respectively.

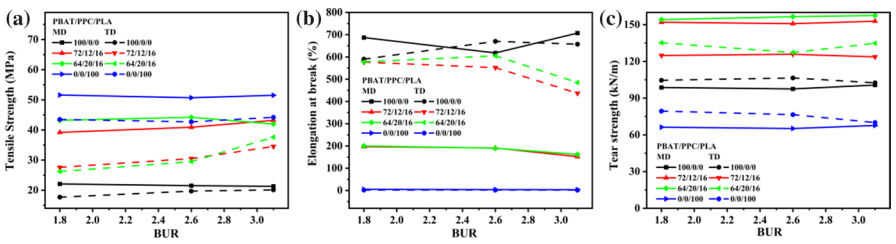

Fig. 1 Mechanical properties of 100/0/0, 72/12/16, 64/20/16 and 0/0/100 PBAT/PPC/PLA mulch films. **a** Tensile strength, **b** Elongation at break, **c** Tear strength

Table 1 Mechanical properties of PBAT/PPC/PLA mulch films (BUR = 3.1)

Sample (wt%) PBAT/PPC/PLA	Tensile Strength (MPa) MD/TD	Elongation at break (%) MD/TD	Tear strength (kN/m) MD/TD
100/0/0	21.3 ± 1.7/20.1 ± 2.3	707.1 ± 97.2/657.2 ± 73.2	100.7 ± 4.5/102.5 ± 6.2
80/20/0	40.0 ± 5.7/30.6 ± 2.9	232.0 ± 31.1/554.6 ± 29.5	169.8 ± 5.1/161.3 ± 6.2
72/20/8	37.1 ± 2.9/28.9 ± 1.9	187.3 ± 12.3/451.5 ± 10.3	153.1 ± 8.1/135.4 ± 9.1
72/12/16	43.2 ± 2.1/34.5 ± 1.2	152.8 ± 24.3/437.6 ± 23.2	152.8 ± 6.3/123.7 ± 5.7
64/28/8	35.8 ± 2.2/31.4 ± 0.9	186.1 ± 17.6/442.1 ± 53.2	169.5 ± 15.0/143.7 ± 6.0
64/20/16	42.0 ± 2.5/37.6 ± 3.4	162.4 ± 54.3/485.3 ± 41.2	157.5 ± 7.7/134.8 ± 17.9
64/12/24	49.8 ± 7.2/37.8 ± 4.4	139.0 ± 29.4/381.3 ± 41.2	109.2 ± 10.7/129.3 ± 17.3
0/0/100	51.5 ± 3.2/44.2 ± 1.5	3.6 ± 0.5/2.0 ± 0.8	67.7 ± 2.5/70.1 ± 3.5

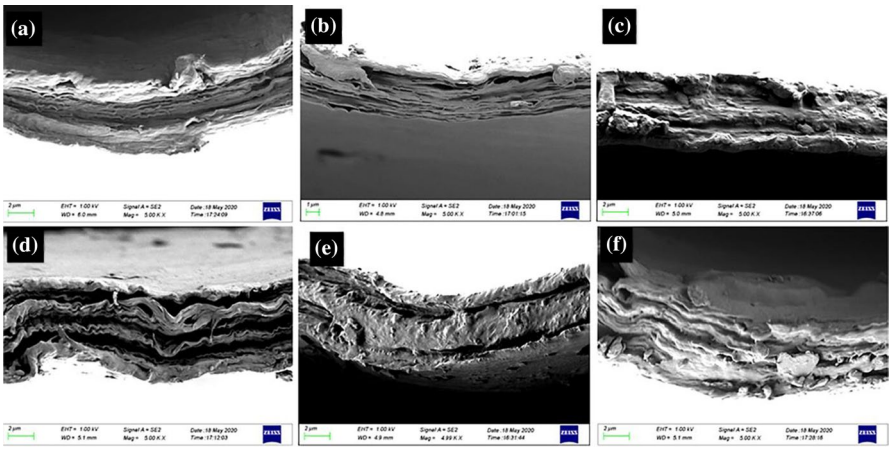

Fig. 2 SEM micrographs of the tear fracture surfaces of PBAT/PPC/PLA films (BUR = 3.1) in MD: **a** 80/20/0, **b** 72/20/8, **c** 72/12/16, **d** 64/28/8, **e** 64/20/16, **f** 64/12/24

The tear strength of the mulch film also showed a trend corresponding to the tensile performance. With the addition of PLA, the tear strength of the film decreased from 169.8/161.3 to 109.2/129.3 kN m^{-1} (MD/TD), respectively.

It was worth mentioning that when the PLA content increases from 16 to 24%, the elongation at break and tear strength of the film showed an accelerated trend of decline, which may be caused by the poor compatibility of the film caused by the higher PLA content [33].

SEM analysis

In order to study the fracture mechanisms responsible for the high tear strength, the tearing fracture surfaces in MD of PBAT/PPC/PLA mulch films were observed by SEM. SEM micrographs were shown in Fig. 2.

Generally speaking, brittle materials would show smooth tearing fracture surface and slight plastic deformation. It can be seen that the tear fracture surfaces of all the 80/20/0 to 64/12/24 PBAT/PPC/PLA mulch films exhibited roughness and had many root-like whiskers and long stretches of ligaments. For the PBAT/PPC/PLA mulch films, obvious matrix deformation and some cavitation structures could be found. In particular, the surface wrinkles of the 64/20/16 and 64/12/24 PBAT/PPC/PLA (Fig. 2e and f) films appeared rougher and exhibited more obvious ductile fracture, which corresponded to its higher tensile strength.

These folds were parallel to the gap, forming clusters of highly stretched material. The cause of the rumples was that there was a big tear at the crack tip before the unstable fracture begins. A large amount of deformation in front of the crack tip created these structures. Notably, the PBAT matrix had obvious large-scale plastic deformation, which meant that the PBAT matrix had undergone shear yield. Corresponding to the mechanical experiment, ductile fracture occurred in the mulch, and the addition of rigid PLA increased the mechanical strength of the mulch film.

DMA

DMA is used to study the mechanical behaviour of materials to analyze the compatibility of blends. The dependence of storage modulus (*E'*) on the temperature of neat PBAT, PPC, PLA, and the ternary blends was shown in Fig. 3a. In the regions between − 60 and − 32 °C, PBAT *E'* was about 2.1 GPa, and as the temperature increased, PBAT appeared glass transition, and *E'* dropped by more than an order of magnitude, as low as 180 MPa.

As the temperature continued to rise, approaching the melting point of PBAT, PBAT *E'* showed a more pronounced drop, as low as 10 MPa. Neat PPC and PBAT showed the same trend, and the difference was that they had different glass transition temperatures (T_g). When the temperature of PLA exceeded 90 °C, *E'* increased significantly, which corresponded to the cold crystallization phenomenon of neat PLA. Compared with neat PBAT, the PBAT/PPC/PLA blends *E'* had higher storage

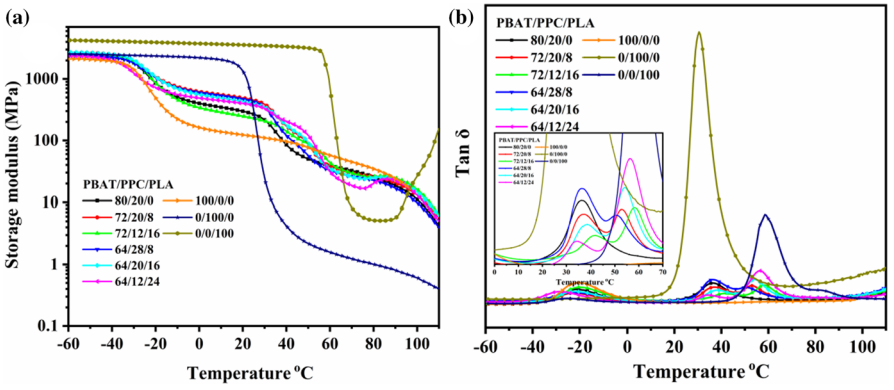

Fig. 3 Dynamic mechanical properties of PBAT/PPC/PLA ternary blends: **a** storage modulus *E'* for − 60 to 110 °C; **b** the loss factor tan*δ* for − 60 to 110 °C;

modulus when the temperature was lower than 30 °C. Additionally, a peak was observed near 87 °C, which was due to the cold crystallization of PLA when the content of PLA was increased to 16%. When the content of PLA was increased to 24%, the peak of cold crystallization of PLA was reduced to 85 °C, indicating that PLA had a certain crystallization ability in the system.

The loss factor (tanδ) is the ratio between the loss modulus (E'') and E'. The tanδ of neat PBAT, PPC, PLA, and the blends was given in Fig. 3b. It could be seen that three tanδ peaks were observed around − 20.6, 30.5 and 59.1 °C for neat PBAT, PPC and PLA, respectively. Due to the addition of flexible PBAT, the value of tanδ of mulch blends was significantly lower than that of neat PLA. Meanwhile, it could be observed that with the increase of PLA and PPC content, the glass transition temperatures of PLA, and PPC approached each other, for the 64/20/16 PBAT/PPC/PLA blend, tanδ peaks of PLA T_g dropped from 59.1 to 54.5 °C, and tanδ peaks of PPC T_g increased from 30.5 to 38.2 °C (Table 2). This result showed that the system showed a certain degree of compatibility, implying that there was better interfacial interaction between PLA and PPC. However, the T_g of PBAT in the blends did move toward low temperature, especially the 64/12/24 PBAT/PPC/PLA blend, which decreased to -28.3 °C. Regarding this phenomenon, it should be that the thermal expansion coefficient of PLA and PPC mixed into the PBAT matrix was different from that of PBAT. When the temperature rose, more free volume was generated inside the blends, which made the PBAT molecular chain easier to move.

Thermal properties

PBAT and PLA are typical semi-crystalline polymers. PPC is an amorphous polymer. Differential scanning calorimetry (DSC) was used to study the thermal properties of PBAT, PPC, PLA and PBAT/PPC/PLA mulch films. The result was shown in Fig. 4. T_g, crystallization temperature (T_c), melting temperature (T_m), the heat of fusion (ΔH_m), crystallinity (X_c) data were listed in Table 3. T_c of neat PBAT was 50.7 °C during the cooling run in Fig. 4a. At the cooling rate of 10 °C/min, no crystallization exothermic peak corresponding to neat PLA was observed, indicating

Table 2 T_g of PPC and PLA in PBAT/PPC/PLA ternary blends

Samples	T_{g1} (°C)	T_{g2} (°C)	T_{g3} (°C)
100/0/0	− 20.6	–	–
0/100/0	–	30.5	–
0/0/100	–	–	59.1
80/20/0	− 21.5	36.4	–
72/20/8	− 22.3	37.1	53.2
72/12/16	− 20.7	42.2	57.5
64/28/8	− 22.3	36.5	50.4
64/20/16	− 22.1	38.2	54.5
64/12/24	− 28.3	34.2	56.5

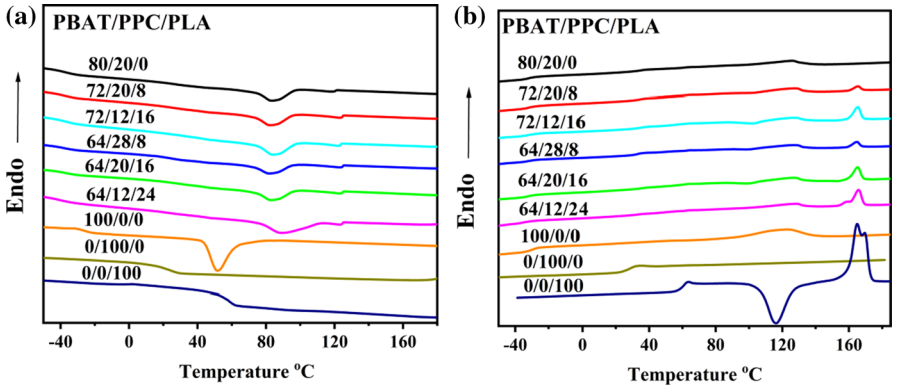

Fig. 4 DSC thermograms for the PBAT/PPC/PLA blends. **a** in the cooling run, **b** in the second heating run

Table 3 Crystallization properties of PBAT/PPC/PLA blend films

Samples (wt%)	T_{g1} (°C)	T_{g2} (°C)	T_{g3} (°C)	T_c (°C)	T_{m1} (°C)	T_{m2} (°C)	ΔH_{m1} (J/g)	ΔH_{m2} (J/g)	X_c (%)
100/0/0	−29.6	–	–	50.7	120.3	–	20.4	–	17.8
0/100/0	–	28.6	–	–	–	–	–	–	–
0/0/100	–	–	61.9	–	–	170.3	–	39.7	–
80/20/0	−31.8	33.7	–	83.1	125.9	–	7.5	–	10.7
72/20/8	−32.2	34.3	61.7	82.3	127.2	165.6	–	1.6	–
72/12/16	−33.2	34.8	61.5	83.8	127.3	165.2	–	5.2	–
64/28/8	−32.2	33.1	61.8	82.0	127.2	164.9	–	2.3	–
64/20/16	−32.2	33.7	61.3	83.1	127.7	165.3	–	5.2	–
64/12/24	−35.7	33.3	61.7	89.3	128.4	165.8	–	7.8	–

that the crystallization rate of neat PLA was slow. For neat PPC, no crystallization behaviour was observed in either the process of heating or cooling.

Comparing with the curves of neat polymers and mulch films, it showed that, T_c of PBAT in mulch films increased from 50.7 to 83.1 °C with increasing PPC content. With increasing PLA content, the T_c of PBAT increased from 83.1 to 89.3 °C, indicating that the addition of PPC and PLA promoted the crystallization of PBAT. Some studies believed that the enhanced mobility of the near-surface chain segment could lead to the improved local order of the near-surface chain [34, 35]. The PBAT/PPC/PLA ternary film system also had a certain degree of compatibility. Therefore, it was speculated that PPC and PLA phases had an accelerated crystallization effect on PBAT. The relatively small content of PLA in the mulch film makes it difficult to observe the crystallization of PLA during cooling.

The glass transition temperatures of neat PBAT, PPC, PLA and mulch films were roughly the same as DMA, but there were some differences in the specific data due to the different measurement mechanisms. In addition, for the melting peak of PBAT

and the cold crystallization peak of PLA, because they were in a similar temperature range, and influenced and covered with each other during the second heating run, it was difficult to analyze and discuss. But in general, adding PLA and PPC to the PBAT matrix reduced the crystallinity of both PBAT and PLA to a certain extent.

Barrier performance

The barrier performance of the mulch film is of great significance in practical applications. The water vapor permeability (WVP) of the mulch films was given in Table 4. It could be seen that the barrier property of neat PBAT was poor, the WVP of PBAT was 20.5×10^{-14} g cm/cm^2·s·Pa. After adding 10 wt% PPC, the WVP of the mulch films dropped rapidly to 12.3×10^{-14} g cm/cm^2·s·Pa. With increasing PPC content from 0 to 28 wt%, the WVP of the mulch films decreased to 8.82×10^{-14} g cm/cm^2·s·Pa. Comparing the WVP of 64/28/8, 64/20/16 and 64/12/24 films, it can be seen that the higher the PPC content, the better the barrier performance of the mulch film, PPC had a more effective effect on improving the barrier properties of mulch films.

PLA could also improve the barrier performance of mulch film. The WVP of neat PLA is 9.52×10^{-14} g·cm/cm^2·s·Pa. After adding 10 wt% PLA, the WVP of the mulch films dropped to 12.9×10^{-14} g·cm/cm^2·s·Pa. Comparing the WVP of 80/20/0, 72/20/8, and 64/20/16 mulch films, with the gradual increase of PLA content, the WVP of the mulch film dropped from 11.7×10^{-14} to 9.02×10^{-14} g·cm/cm^2·s·Pa, which was even lower than that of neat PLA. Combining the previous discussion, this might be due to the better compatibility between PLA and PPC. When the contents of PPC and PLA were close to each other, the entanglement degree between polymer molecular chains increased, which decreased the permeation path of gas

Table 4 Water vapor barrier properties of PBAT/PPC/PLA mulch films

PBAT/PPC/PLA	Water Vapor Transmission g/(m^2·day)	Water Vapor Permeability $\times10^{-14}$ g·cm/cm^2·s·Pa
100/0/0	1534.5	20.5
90/10/0	759.68	12.3
90/0/10	775.37	12.9
80/10/10	562.23	11.9
80/20/0	671.02	11.7
72/20/8	437.67	10.2
72/12/16	451.01	11.4
64/28/8	379.07	8.82
64/20/16	368.82	9.02
64/12/24	423.08	9.30
0/0/100	2725.5[a]	9.52

[a]The thickness of neat PLA is much larger than that of mulch, so it has a larger WVT

molecules. Improving the barrier performance is conducive to water and moisture conservation of the mulch films is conducive to the healthy growth of crops.

Light stability

It can be seen that the addition of light stabilizers did not significantly change the mechanical properties of the mulch (Table S2**,** Supporting Information). After the 100-h UV aging test, it could be seen that there were apparent changes between different samples (Fig. 5). Among them, the samples without UV-770, the elongation at break only reached 38.6%/15.3% (MD/TD), a transition from toughness to brittleness occurred, and the tensile strength was also significantly reduced to 23.8 MPa/14.0 MPa (MD/TD).

While the sample with a UV-770 mass fraction of 1%, although the tensile strength had also been significantly reduced, the elongation at break still exceeded 150%/234% (MD/TD), showing ductile fracture. Under the action of HALS, the mulch film samples obtained good light stability. Excellent UV resistance is very important for mulch films, which is beneficial to improve the service life of the biodegradable films.

FTIR results

HALS protects the polymer coating from photooxidative damage by forming nitrogen oxide free radicals, which then consume the destructive free radicals in a process called the Denisov cycle. However, the exact mechanism of this process has always been controversial. A dozen different reaction pathways and more than 30 individual reactions have been proposed in the literature [29, 36, 37].

In order to study the ultraviolet aging and light stabilizer mechanism of the mulch film, infrared spectroscopy experiments were carried out. FTIR spectra and data of PBAT/PPC/PLA/UV-770 blends were shown in Fig. 6. The two peaks near

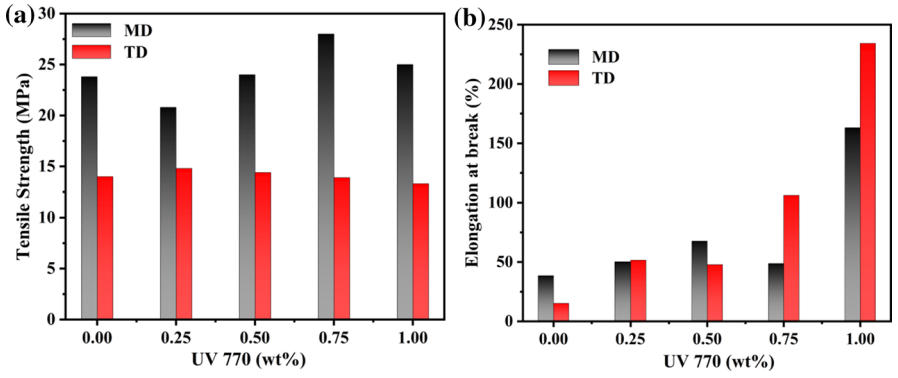

Fig. 5 Effects of different contents of UV-770 on the mechanical properties of 64/20/16 PBAT/PPC/PLA mulch films after degradation by UV irradiation

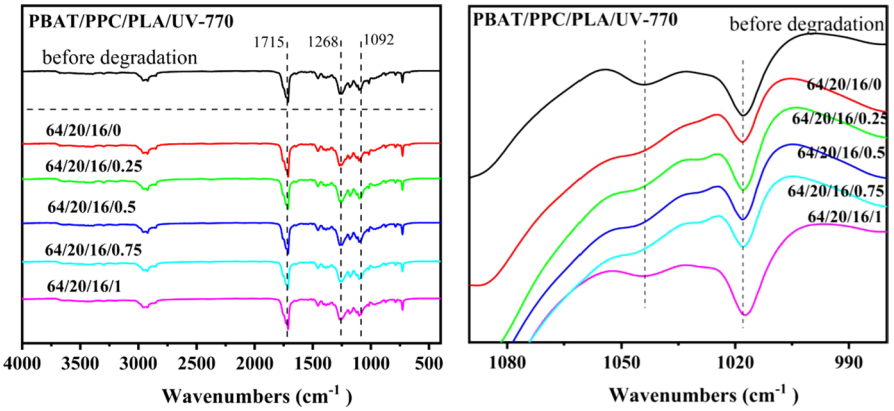

Fig. 6 FTIR spectra of PBAT/PPC/PLA/UV-770 mulch films

1758 and 1715 cm^{-1} in the infrared spectrum corresponded to the crystalline and amorphous carbonyl (C=O) stretching vibrations of the carbonyl group of PBAT, respectively. The two peaks at 1268 and 1252 cm^{-1} respectively corresponded to the C-O bond stretching vibration in the amorphous and crystalline regions of PBAT. The spectra show characteristic ester absorption peaks at 1092, 1129 and 1184 cm^{-1} for the stretching vibration of the C–O of PLA. After comparing peak position and peak height, we found a more obvious difference between the characteristic –C–O– stretching vibration peaks of PBAT at 1042 cm^{-1} and 1018 cm^{-1}. With increasing light stabilizer content, the characteristic peak gradually increased. It indicated that the addition of UV-770 could effectively protect the –C–O– bond of PBAT from breaking. Therefore, it can be concluded that the breakdown of the ester bond of the main chain of PBAT is the main cause of polymer degradation, and UV-770 can effectively protect PBAT from photodegradation.

Conclusions

In this paper, fully biodegradable PBAT/PPC/PLA mulch films were prepared by extrusion blending and blown film to obtain high-performance materials with good application value. The 3.1 BUR mulch film was better in mechanical properties. The 64/20/16 PBAT/PPC/PLA mulch film showed good mechanical properties. The tensile strength was as high as 43.0 MPa/37.6 MPa (MD/TD), the elongation at break reached 160%/450% (MD/TD), and the tear strength could reach 140 kN m^{-1}. It showed that the PBAT/PPC/PLA mulch film had partial compatibility from DMA and DSC analysis. The DSC results showed that the crystallinity of PBAT in the mulch was low, and it was also tricky for PLA with less content to form perfect crystals. Due to the addition of PPC, the mulch had good barrier properties. After adding high-efficiency hindered amine light stabilizers, the mulch film obtained good light stability, and its elongation at break still exceeded 100% after 100 h of UV irradiation. The rupture of the ester bond of the PBAT backbone in the mulch is

the main cause of polymer degradation, and HALS UV-770 can effectively protect PBAT from photodegradation. Good mechanical properties, excellent barrier properties, good light stability, and complete biodegradability are all essential for mulch films. Biodegradable mulch plays an important role in protecting the environment and replacing non-renewable resources. This result provides a reference for the following research on the design, production, application and promotion of biodegradable mulch films.

Supplementary Information The online version contains supplementary material available at https://doi.org/10.1007/s00289-022-04173-7.

Acknowledgements This work was supported by the Science and Technology Development Plan of Jilin Province (20210203199SF), Science and Technology Services Network Program of Chinese Science Academy (No. KFJ-STS-ZDTP-082), Chinese Science Academy (Changchun Branch) (No. 2020SYHZ0002 and No. 2020SYHZ0047), and the National Science Foundation of Zhejiang Province of China (No. LQY19B040001).

References

1. Kasirajan S, Ngouajio M (2012) Polyethylene and biodegradable mulches for agricultural applications: a review. Agron Sustain Dev 32(2):501–529
2. Steinmetz Z, Wollmann C, Schaefer M, Buchmann C, David J, Tröger J, Muñoz K, Frör O, Ellen G (2016) Plastic mulching in agriculture. Trading short-term agronomic benefits for long-term soil degradation? Sci Total Environ 550:690–705
3. Sintim HY, Flury M (2017) Is biodegradable plastic mulch the solution to agriculture's plastic problem? Environ Sci Technol 51(3):1068–1069
4. Barragán DH, Pelacho AM, Martin-Closas L (2016) Degradation of agricultural biodegradable plastics in the soil under laboratory conditions. Soil Res 54(2):216–224
5. Miles C, Wallace R, Wszelaki A, Martin J, Cowan J, Walters T, Inglis D (2012) Deterioration of potentially biodegradable alternatives to black plastic mulch in three tomato production regions. HortScience 47(9):1270–1277
6. Abd El-Rahman KM, Ali SAF, Khalil AI, Kandil S (2020) Influence of poly(butylene succinate) and calcium carbonate nanoparticles on the biodegradability of high density-polyethylene nanocomposites. J Polym Res 27(8):1–21
7. Ali SFA, Elsad RA, Mansour SA (2021) Enhancing the dielectric properties of compatibilized high-density polyethylene/calcium carbonate nanocomposites using high-density polyethylene-g-maleic anhydride. Polym Bull 78:1393–1405
8. Ali SFA (2016) Mechanical and thermal properties of promising polymer composites for food packaging applications. In Iop Conf Ser 137: 012035
9. El-Rafey E, Walid WM, Syala E, Ezzat AA, Ali SFA (2021) A study on the physical, mechanical, thermal properties and soil biodegradation of HDPE blended with PBS/HDPE-g-MA. Polym Bull online.
10. Touchaleaume F, Martin-Closas L, Angellier-coussy H, Chevillard A, Cesar G, Gontard N, Gastaldi E (2016) Performance and environmental impact of biodegradable polymers as agricultural mulching films. Chemosphere 144:433–439
11. Bilck AP, Grossmann MVE, Yamashita F (2010) Biodegradable mulch films for strawberry production. Polym Test 29(4):471–476
12. Jia SL, Chen YJ, Yu YL, Han LJ, Zhang HL, Dong LS (2019) Effect of ethylene/butyl methacrylate/glycidyl methacrylate terpolymer on toughness and biodegradation of poly (L-lactic acid). Int J Biol Macromol 127:415–424
13. Lu JM, Qiu ZB, Yang WT (2007) Fully biodegradable blends of poly(l-lactide) and poly(ethylene succinate): miscibility, crystallization, and mechanical properties. Polymer 48(17):4196–4204

14. Jiang L, Wolcott MP, Zhang JW (2006) Study of biodegradable polylactide/poly(butylene adipate-co-terephthalate) blends. Biomacromol 7(1):199–207
15. Ma P, Cai X, Zhang Y, Wang S, Dong W, Chen M, Lemstra PJ (2014) In-situ compatibilization of poly(lactic acid) and poly(butylene adipate-co-terephthalate) blends by using dicumyl peroxide as a free-radical initiator. Polym Degrad Stab 102:145–151
16. Yeh JT, Tsou CH, Huang CY, Chen KN, Wu CS, Chai WL (2010) Compatible and Crystallization properties of poly(lactic acid)/poly(butylene adipate-co-terephthalate) blends. J Appl Polym Sci 116(2):680–687
17. Li K, Peng J, Turng LS, Huang HX (2011) Dynamic rheological behavior and morphology of polylactide/poly(butylenes adipate-co-terephthalate) blends with various composition ratios. Adv Polym Tech 30(2):150–157
18. Chiu HT, Huang SY, Chen YF, Kuo MT, Chiang TY, Chang CY, Wang YH (2013) Heat treatment effects on the mechanical properties and morphologies of poly (lactic acid)/poly (butylene adipate-co-terephthalate) blends. Int J of Polym Sci 2013:951696
19. Pietrpsanto A, Scarfato P, Di Maio L, Nobile MR, Incarnato L (2020) Evaluation of the suitability of poly(lactide)/poly(butylene-adipate-co-terephthalate) blown films for chilled and frozen food packaging applications. Polymers 12(4):804
20. Coban O, Bora MO, Kutluk T, Ozkoc G (2018) Mechanical and thermal properties of volcanic particle filled PLA/PBAT composites. Polym Compos 39:E1500–E1511
21. Yu YL, Xu PF, Jia SL, Pan HW, Zhang HL, Wang DM, Dong LS (2019) Exploring polylactide/poly(butylene adipate-co-terephthalate)/rare earth complexes biodegradable light conversion agricultural films. Int J Biol Macromol 127:210–221
22. Okada M (2002) Chemical syntheses of biodegradable polymers. Prog Polym Sci 27(1):87–133
23. Luinstra GA (2008) Poly(propylene carbonate), old copolymers of propylene oxide and carbon dioxide with new interests: catalysis and material properties. Polym Rev 48(1):192–219
24. Shi XD, Gan ZH (2007) Preparation and characterization of poly(propylene carbonate)/montmorillonite nanocomposites by solution intercalation. Eur Polym J 43(12):4852–4858
25. Zheng F, Mi QH, Zhang K, Xu J (2016) Synthesis and characterization of poly(propylene carbonate)/modified sepiolite nanocomposites. Polym Compos 37(1):21–27
26. Kijchavengkul T, Auras R, Rubino M, Selke S, Ngouajio M, Fernandez RT (2011) Formulation selection of aliphatic aromatic biodegradable polyester film exposed to UV/solar radiation. Polym Degrad Stab 96(10):1919–1926
27. Kijchavengkul T, Auras R, Rubino M, Ngouajio M, Fernandez RT (2008) Assessment of aliphatic-aromatic copolyester biodegradable mulch films. Part I: Field study. Chemosphere 71(5):942–953
28. Kijchavengkul T, Auras R, Rubino M, Ngouajio M, Fernandez RT (2008) Assessment of aliphatic-aromatic copolyester biodegradable mulch films. Part II: Laboratory simulated conditions. Chemosphere 71(9):1607–1616
29. Hodgson JL, Coote ML (2010) Clarifying the mechanism of the denisov cycle: How do hindered amine light stabilizers protect polymer coatings from photo-oxidative degradation? Macromolecules 43(10):4573–4583
30. Souza PMS, Sommaggio LRD, Marin-Morales MA, Morales AR (2020) PBAT biodegradable mulch films: Study of ecotoxicological impacts using Allium cepa, Lactuca sativa and HepG2/C3A cell culture. Chemosphere 256:126985
31. Souza PMS, Morales AR, Sanchez EMS, Mei LHI (2018) Study of PBAT photostabilization with ultraviolet absorber in combination with hindered amine light stabilizer and vitamin E, aiming mulching film application. J Polym Environ 26(8):3422–3436
32. Su ZZ, Li QY, Liu YJ, Hu GH, Wu CF (2009) Compatibility and phase structure of binary blends of poly(lactic acid) and glycidyl methacrylate grafted poly(ethylene octane). Eur Polym J 45(8):2428–2433
33. Wang XY, Pan HW, Jia SL, Cao ZW, Han LJ, Zhang HL, Dong LS (2020) Mechanical properties, crystallization and biodegradation behavior of the polylactide/poly(3-hydroxybutyrate-co-4-hydroxybutyrate)/poly(butylene adipate-co-terephthalate) blown films. Chin J Polym Sci 38(10):1072–1081

34. Roth CB, McNerny KL, Jager WF, Torkelson JM (2007) (2007) Eliminating the enhanced mobility at the free surface of polystyrene: fluorescence studies of the glass transition temperature in thin bilayer films of immiscible polymers. Macromolecules 40(7):2568–2574
35. Factor BJ, Russell TP, Toney MF (1991) Surface-induced ordering of an aromatic polyimide. Phys Rev Lett 66(9):1181–1184
36. Allen NS (1986) Recent advances in the photooxidation and stabilization of polymers. Chem Soc Rev 15(3):373–404
37. Step EN, Turro NJ, Klemchuk PP, Gande ME (1995) Model studies on the mechanism of hals stabilization. Angew Makromol Chem 232:65–83